Supplementary Information for

Large earthquake proximity indicated by Seismic moment efficiency and frequency-number distribution of Small Earthquakes

Satoshi Matsumoto

Institute of Seismology and Volcanology, Kyushu University

Contents of this file

Introduction

We provide additional text and figures to support the main text. Text S1 describes the moment-tensor stacking used in this study. The figures show additional information regarding the b-value estimation, detailed results for the hypocentral area of the 2016 Kumamoto earthquake, and the Mstk/M0 behavior for various friction coefficients and strass ratios.

Text S1.

We show that stacked moment tensor rotated angle $\pm\theta$ from the principal stress direction returns to the original shape of the tensor with a different magnitude. Consider the case in which the moment tensor (M) has a shape identical to that of a stress tensor. If M is rotated by an angle θ, the rotation tensor (R) becomes:

$$\mathrm{M} = \begin{pmatrix} 1 & 0 & 0 \\ 0 & 0 & 0 \\ 0 & 0 & -1 \end{pmatrix} \tag{A1}$$

$$\mathrm{R} = \begin{pmatrix} \cos(\theta) & 0 & -\sin(\theta) \\ 0 & 0 & 0 \\ \sin(\theta) & 0 & \cos(\theta) \end{pmatrix} \tag{A2}$$

The rotated tensor M’ is the RMR^T, where superscript T indicates the matrix transpose. If we choose angle $\theta = -\theta$, the rotation tensor R’ is equal to R^T. Summing the rotated moment tensor with θ to that with −θ, we obtain the tensor M’’ as follows:

$$M'' = RMR^T + R'MR'^T = RMR^T + R^TMR = \begin{pmatrix} 2\cos(\theta)^2 - 2\sin(\theta)^2 & 0 & 0 \\ 0 & 0 & 0 \\ 0 & 0 & -2\cos(\theta)^2 + 2\sin(\theta)^2 \end{pmatrix} \quad (A3)$$

Therefore, the stacked moment tensor has the same shape as M. If the fault planes are randomly distributed in a volume, the stacking moment tensors may have an identical shape to M because pairs of fault planes with positive and negative rotation angles θ are found. We note that the stacked M for a large number of events can be close to the tensor shape of the deviatoric stress tensor, as suggested by Matsumoto (2016), based on the flow rule in plasticity theory. However, this effect was minor in the present study.

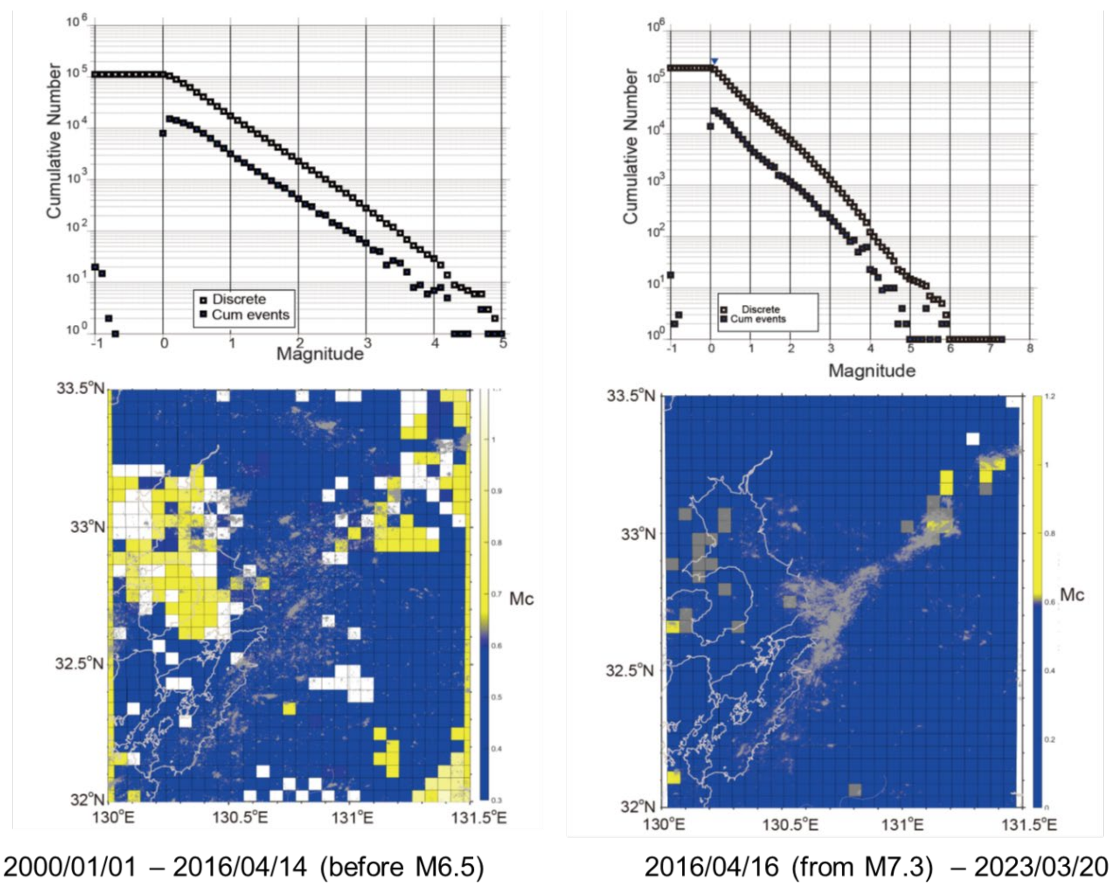

Figure S1. Frequency–magnitude distribution for periods 1 and 2, and Mc (lower limit of distribution of the range satisfying the Gutenberg–Richter relationship) distribution estimated by the ZMAP software. Upper panels show the distribution. Open and solid squares indicate the cumulative and discrete number of events within a magnitude range with an interval of 0.1, respectively. Lower panels show the Mc distribution. Segment Mc > 0.6 is colored yellow. Most of the area in the target region indicates an Mc of < 0.6.

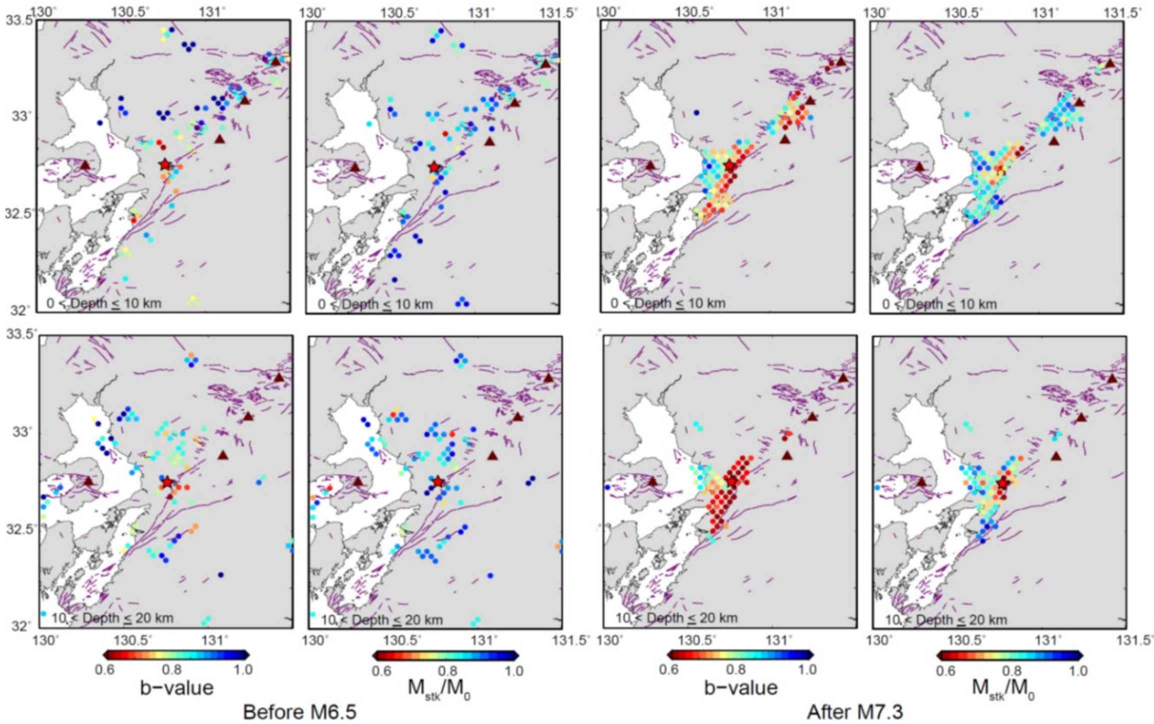

Figure S2. Individual plots of the b value and Mstk/M0 for two depth ranges and two periods (Figure 3).

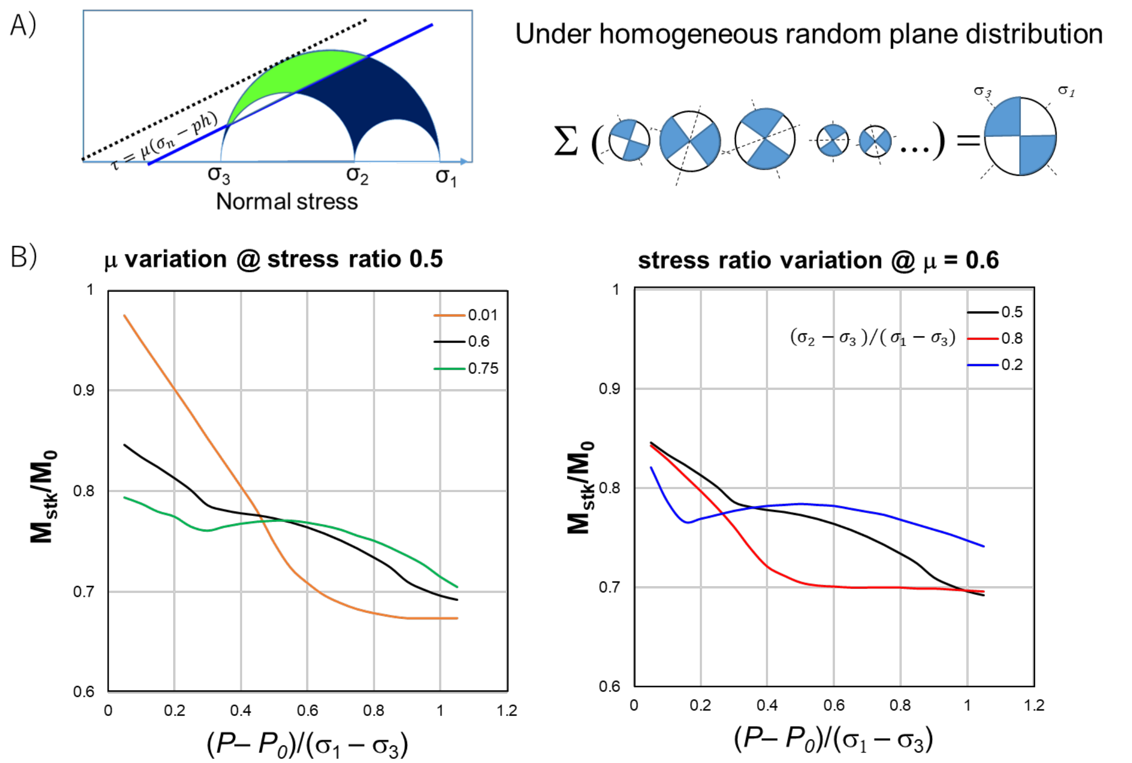

Figure S3. Mstk/M0 variation under homogeneous random fault plane distribution. The variation is calculated by following steps: 1) set fault plane normal vectors for all direction to be homogeneous; 2) calculate shear and normal stress on each fault under the assumed stress field; 3) select fault planes in the pore pressure range from P_0 to P of the Mohr circle; 4) stack moment tensors for the selected planes; 5) obtain Mstk/M0 for each P and stress ratio. A) Schematic illustration of the relationship between the Mohr circle and CFF, and stacking moment tensor. B) Mstk/M0 change for p variation. Left panel shows the variation for friction coefficients μ = 0.01, 0.6, and 0.75 with fixed stress ratio $(\sigma_2 - \sigma_3)/(\sigma_1 - \sigma_3)$ of 0.6. Right panel displays that for stress ratios of 0.5, 0.8, and 0.2 with fixed μ = 0.6.

References

Matsumoto, S. (2016). Method for estimating the stress field from seismic moment tensor data based on the flow rule in plasticity theory. *Geophysical Research Letters*, *43*(17), 8928–8935. https://doi.org/10.1002/2016GL070129